To appear in *High Pressure Research*
Vol. 00, No. 00, Month 20XX, 1–12

Modified Bridgman anvils for high pressure synthesis and neutron scattering

Bianca Haberl[a]*, Jamie J. Molaison[a], Joerg C. Neuefeind[a], Luke L. Daemen[a], and Reinhard Boehler[a,b]

[a] *Neutron Scattering Division, Neutron Sciences Directorate, Oak Ridge National Laboratory, Oak Ridge, TN 37831, USA*;
[c] *Geophysical Laboratory, Carnegie Institution for Science, Washington, DC 20015, USA*

(*Received 00 Month 20XX; final version received 00 Month 20XX*)

A simple modified Bridgman design for large volume pressure anvils usable in the Paris-Edinburgh press has been demonstrated at Oak Ridge National Laboratorys Spallation Neutron Source. The design shows advantages over the toroidal anvils typically used in the Paris-Edinburgh press, mainly rapid compression/decompression rates, complete absence of blow-outs upon drastic phase transitions, simplified cooling, high reliability, and relative low loads (∼40 tons) corresponding to relatively high pressures (∼20 GPa). It also shows advantages over existing large-volume diamond cells as sample volumes of ∼2-3 mm^3 can be easily and rapidly synthesized. The anvils thus allow sample sizes sufficient for *in situ* neutron diffraction as well as rapid synthesis of adequate amounts of new materials for *ex situ* analysis via total neutron scattering and neutron spectroscopy.

Keywords: High pressure neutron scattering, high pressure materials synthesis, pure amorphous silicon and germanium

*Corresponding author. Email: haberlb@ornl.gov

1. Introduction

Neutron scattering is a powerful tool for the study of materials. Neutrons can directly probe many low Z elements such as hydrogen, oxygen or carbon, can interact with the magnetic moment and offer simplified direct analytical computations of neutron spectroscopic data (see, for example, Ref. [1]). Neutron scattering thus gives a complementary insight into materials' behaviours at ambient conditions and also under extreme conditions such as high pressure. High pressure neutron scattering requires, however, larger sample volumes than other high pressure techniques. Standard diamond anvil cells (DACs) can reach several Mbar (1 Mbar = 100 GPa), but sample volumes are too small, in the order of 0.0001 mm^3 only, for neutron scattering. Consequently, the vast majority of high pressure devices for neutrons are designed for sample volumes typically in the order of 1-100 mm^3, volumes which allow for 20 GPa or less.

Such large-volume neutron pressure cells are also very useful for materials synthesis. Naturally, the large volumes that can be pressurized also result in large sample volumes that can be recovered for further uses or analyses. A prime example here are the toroidal and Chechevitsa ('lentil') designs developed from the 1960s onward in the former Soviet Union [2]. These designs are based on depressions or 'dimples' in the centre of flat anvils often surrounded by a toroid for additional gasket support and have been extensively used for high pressure materials synthesis.

An extensive body of work has later demonstrated the use of Paris-Edinburgh (PE) presses and such toroidal anvils for various applications of *in situ* neutron scattering at high and low temperature [see Ref. [3] and Refs. therein]. Typically, single-toroidal anvils made from cubic boron nitride (cBN) with sample volumes $\leq$87 mm^3 reach reliably 10 GPa. While double-toroidal anvils made from polycrystalline diamond (PCD) with sample volumes of $\leq$31 mm^3 have achieved close to 30 GPa [4], reliable operation is typically limited to $\sim$18 GPa. A more recent work has further developed the double-toroidal PCD anvil to pressures beyond 22 GPa while allowing for cooling down to 1.8 K [5]. Further work on anvil designs has also employed different materials such as tungsten carbide (WC) or ceramic anvils. While maintaining the central depression or even an additional toroid, nickel-bound WC anvils have improved neutron diffraction intensity by a factor of 2-3 [6]. Moreover, the use of ceramic anvils with similar central depressions and toroids has improved diffraction intensity further by an order of magnitude [7].

Another approach to large-volume high pressure studies for sample synthesis or *in situ* neutron scattering is based on multi-anvil designs in large volume presses (often up to 1000 ton) [8]. This approach also allows for simultaneous heating to several 1000 K [8]. A relatively recent design has thereby achieved a record of 100 GPa at 1500 K on a sample volume in the order of 0.05 mm^3 [9]. Similar designs with larger sample volumes are also being developed for pulsed neutron sources with pressure/temperature conditions of 10 GPa/2000 K or even 16 GPa/1273 K [10, 11].

Higher pressures or also better combination with other extremes such as low temperatures or magnetic fields have been achieved with diamond-anvil type cells adapted for neutron diffraction. For example, a hybrid-anvil-type high-pressure device based on a sapphire and a WC anvil is capable of up to 5 GPa and has been cooled to 1.4 K at 6 T [12, 13]. In this case, the sample chamber was increased through a hemispherical indentation, or 'dimple', in the WC anvil. Moreover, diamond and sapphire cells based on work by Somenkov *et al.* and later Goncharenko *et al.* achieved up to $\sim$40 GPa [14, 15]. Particularly, for the sapphire anvils, sample volumes were increased through a central hole or 'dimple'. Further development at the Spallation Neutron Source (SNS), using single crystal diamonds and composite seats has achieved a record pressure of 94 GPa [16] on a sample volume of $\sim$0.02 mm^3. More recently, continued work at the SNS achieved 45 GPa on a sample volume of 0.16 mm^3 using single crystal diamond anvils [17] and 10 GPa on

$\sim$1.5 mm^3 using anvils made from a form of polycrystalline diamond [18]. Note that in the PCD case, sample volumes were also increased through a central 'dimple'.

However, the many cells that exist currently are not necessarily adapted to rapid turn-around as useful for pressure synthesis, often do not allow for good control over (de)compression rates and also do not readily cover the low temperature regime. Furthermore, synthesis from maximum pressures of 20 GPa or beyond is also not easily available.

In this present work, we contribute to overcome this short coming. We describe an anvil design for the PE press that accommodates 2-3 mm^3 of sample volume. These anvils are capable of reaching 20 GPa tens of times without failure. In particular they require significantly less load compared to traditional toroidal PE anvils. Furthermore, they can be more easily cooled to 90 K (within 30 mins) and can be decompressed rapidly within $\sim$1 s. Such control over decompression parameters (temperature, decompression rate) is critical for many syntheses processes as shown here on the examples of amorphous silicon and germanium. Furthermore, the sample volume is sufficient for *in situ* diffraction on SNS's high pressure beamline SNAP [19]. In the case of amorphous Ge, the sample volume synthesized through high pressure, low temperature is also sufficient for *ex situ* neutron diffraction on SNS's NOMAD beamline [19, 20] as well as *ex situ* inelastic neutron scattering on SNS's VISION spectrometer [21].

2. Anvil Design

The anvil design consists of a simple 0.33 mm deep, 2.5 mm diameter 'dimple' made in the centre of a 4 mm diameter flat top of a PCD anvil as used for the PE press. This is shown in Fig. 1. The opening angle of the two anvils with gasket is $\pm 7°$. The anvil material arrives co-sintered with a tungsten carbide (WC) support ring from Sandvik. This assembly has a 1.5° taper, which facilitates press fitting into a maraging steel support ring with a matching taper. The interference between the two pieces is sufficient to provide $\sim$0.75 GPa of radial support to the anvil after full press fit (with $\sim$6 tons). It should be noted that no consistency exists in the literature in terminology and a large variety of terms is used, e.g. 'non-toroidal', 'cup', 'centre hole', 'hemispherical indentation', 'depression' or 'recession'. These all appear equivalent to our use of 'dimple' here.

Several iterations in gasket preparation revealed an optimized process for sufficient anvil support and gasket friction. In a first step, a flat T301 stainless steel gaskets (1 mm height, 10 mm outer diameter) is aligned concentrically with the dimple and pre-compressed to 12 tons. This results in plastic deformation of the gasket which takes on the shape of the dimples. A hole in then drilled through the gasket centre to form the gasket chamber (with 1.6 mm diameter, height of 1.2 mm). It is important to note that the hole diameter is smaller than the 'dimple' to allow a gasket rim to remain. This rim enables easy realignment of the gasket into the 'dimple' and ensures that the gasket material flows into the 'dimple' during compression. This appears critical to prevent 'blow-outs' and other gasket failures. This set-up results in an empty volume of the gasket chamber of 3.01 mm^3. Since no full packing can be achieved for solid samples as used here later, the volume of resulting synthesized material is $\sim$2 mm^3 in the current case.

This anvil/gasket set-up was used predominantly in the VX5 model of the PE press, a 130 ton press. For offline synthesis, WC backing plates without holes were used to add stability to the anvils. For cooling, disks of G-10 laminate were placed between backing plates and cell body to isolate the PE press from the anvils to-be-cooled for synthesis. Furthermore, a modified backing plate was used that adds a cryogenic reservoir around

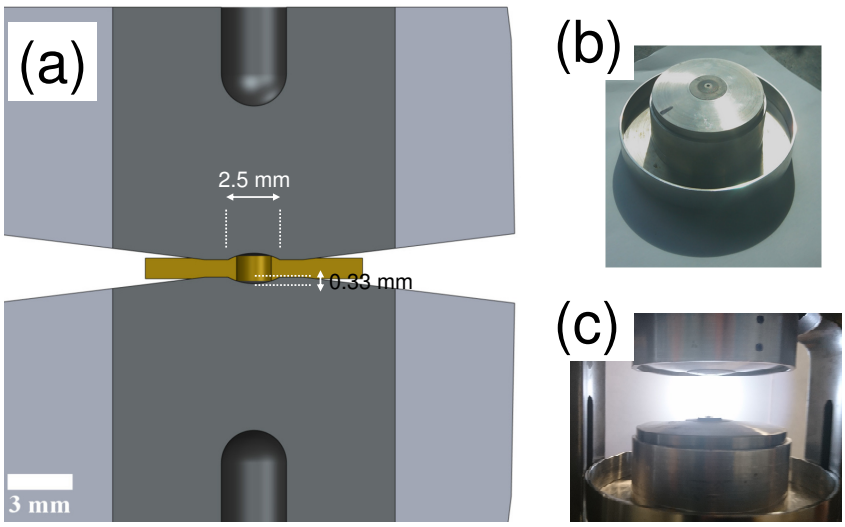

Figure 1. (Colour online) (a) Schematic of the modified Bridgman anvil shown here with the PCD insert and the WC support ring as obtained commercially together with the corresponding stainless steel gasket. The 'dimple' has a depth of 0.33 mm and a diameter of 2.5 mm, the gasket chamber is 1.6 mm diameter by 1.2 mm height resulting in a empty volume of 3.01 mm^3. (b) and (c) Photos of the anvil in its binding ring on a backing plate in the cryogenic reservoir and of the anvil and gasket set up in the press, respectively.

the bottom anvil to facilitate direct cooling with liquid nitrogen (see Fig. 1(b)).

3. *In situ* neutron diffraction on SNAP

The anvil were used for *in situ* diffraction of Group IVa materials (C, Si, Ge) on SNAP [19]. These measurements were predominantly required to extract a pressure-load curve via equation-of-state measurements needed for the later synthesis. Note that an alternative method for pressure calibration of the anvil design described here has been developed by M. Guerette, T.A. Strobel *et al.* as described elsewhere.

For the equation-of-state (EoS) measurements, standard SNAP diffraction settings were used (i.e. both detectors at 90°, chopper frequency of 60 Hz, centre wavelength $\lambda = 2.1$ Å resulting in $d_{max} = 3.2$ Å). In contrast to the standard SNAP set-up, the VX5 PE press was placed in horizontal geometry (i.e. incident beam through anvil). This was necessary since the gasket scatter would have been prohibitively high in a vertical geometry (i.e. incident beam through gasket). The beam was collimated along the entirety of the cell, i.e. through a PE backing plate with a hole and into the synthesis anvil itself using a hollowed-out hexagonal BN (hBN) rods with a final diameter of 1 mm. Accounting for SNAP's divergence, this aims to illuminate as much as sample as possible but to prevent gasket scatter. Prior to compression, this set-up excluded all diffraction from the stainless steel gasket, but some gasket scatter was detected at high pressures.

In situ diffraction data for EoSs were measured on SNAP from crystalline diamond-cubic (dc) Si mixed with lead as pressure calibrant and crystalline dc-Ge. Using the conventional toroidal PE anvil set-up on SNAP always resulted in major 'blow-outs' when Si or Ge were pressurized. This is most likely due to the large volume change ($\geq$20%) that occurs upon metallization of Si and Ge [22]. In contrast, no such blow-out occurred with the present anvil design.

The first two EoS were obtained from one simultaneous measurement of silicon and lead. Therefore, Si powder (NIST, SRM 640d) was mixed with lead powder (Aldrich, -325 mesh, $\geq$99% trace metals basis) in a mixture of 50:50 wt%. The mixed Si:Pb sam-

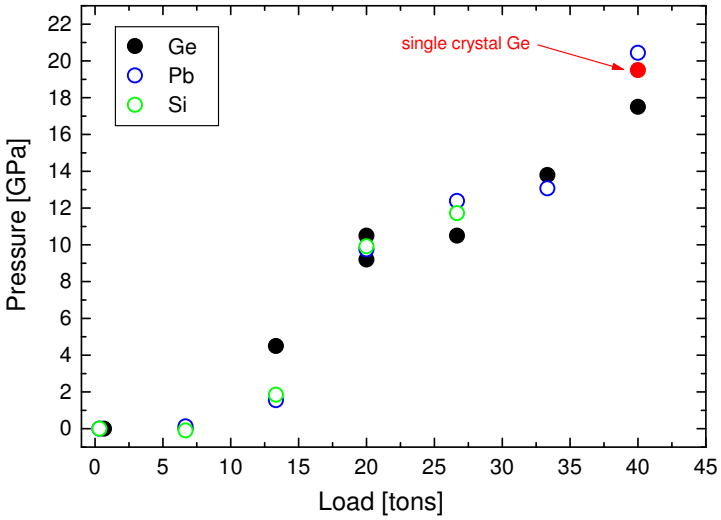

Figure 2. (Colour online) Pressure-load curves obtained from two runs with pure crystalline Ge (closed circles) and one run with crystalline Si in mixture with lead (open circles). Note that the size of each point corresponds to ∼0.5 GPa height, which is larger than the relative error of each pressure determination.

ple was pelletized and loaded into the gasket without a pressure medium. The cell was compressed to 40 t (600 bar in the VX5) while *in situ* diffraction data were collected in 100 bar (=6.7 ton) steps. These diffraction data were reduced to 1D-profiles using Mantid [23]. The pressure-load curve was determined from the EoS of Pb as well as Si. For Pb, a third-order Birch-Murnaghan EoS and the moduli discussed in Ref. [24] were used (B_0=43.2 GPa/B_0'=4.87 for the fcc phase and B_0=46.63 GPa/B_0'=5,23 for the hcp phase). At lower pressures, the Si(111) peak of the dc phase was used as confirmation (B_0=97.8 GPa/B_0'=4.1 and a Vinet EoS [25]). At pressures above ∼11 GPa, Si undergoes a transition to a highly densified metallic phase with white tin, (β-Sn), structure followed by an orthorhombic *Imma* and a simple-hexagonal (sh) phase [26]. The use of these metallic phases for pressure determination was not possible since one of their key signature diffraction peaks disappears beneath the (111) diamond peak. At the highest load, it was confirmed that re-alignement of the cell position along the beam did not yield a change in measured lattice parameters within the resolution limit of SNAP. The resulting pressure-load curves are shown in Fig. 2.

Further EoS were then obtained from germanium. A Ge wafer (University wafer, (100), undoped with $\geq$50 Ωcm^{-1}) was powderized using a mortar and pestle. A portion of a pellet made from resulting fine powder was placed within a gasket chamber. A second gasket was filled with 5-10 single crystal pieces of such Ge. Both samples were equally compressed to 40 t and the EoS of Ge was used to determine the pressure. As for Si, dc Ge undergoes metallization at ∼11 GPa to the (β-Sn) structure [22]. To obtain a consistent pressure reading, the V/V_0 data obtained by Olijnyk [27] under equally non-hydrostatic conditions were used for dc-Ge and (β-Sn)-Ge. For the single crystal pieces only the highest pressure point was obtained in order to confirm a similar pressure-load curve for the potentially somewhat altered packing fraction and shear component. These resulting pressure-load curves are also shown in Fig. 2.

From these pressure-load curves, it is clear that initial load increase does not increase sample pressure. This shows that the gasket material does not deform plastically until above ∼10 t. Pressure then increases swiftly until the pressure load-curve becomes rather flat between 20-30 t for the samples used here. This is due to the fact that Si and Ge both exhibit the same phase transition to metallic phases above ∼11 GPa [22]. This transition

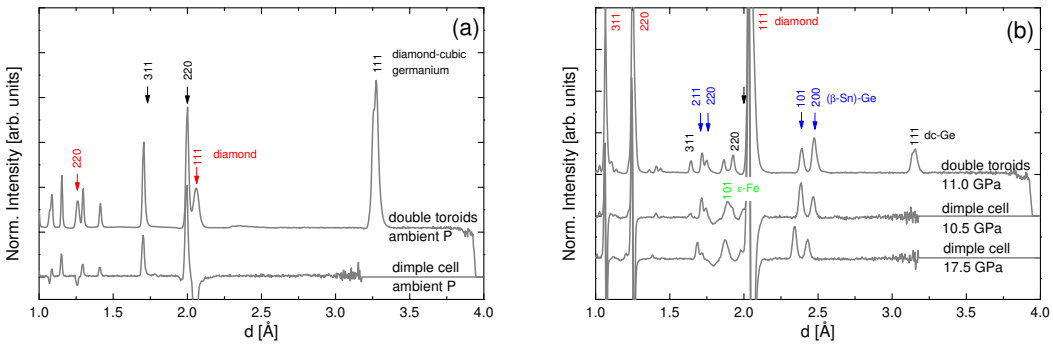

Figure 3. (Colour online) *In situ* diffraction data from dc-Ge taken from the modified Bridgman design compared to the standard double toroidal design at (a) ambient pressure and (b) above 10 GPa.

is accompanied by a ∼20% volume change and is very sluggish for Si [28]. While the same sluggishness has not been noted for Ge in the literature previously, it appears present in the current experiment. Thus, increase of load does not result in much pressure increase but in a continuous transition from the dc phases to the (β-Sn) phases here. Once the transition is completed, pressure increases again at a similar rate as prior to the onset of the transition.

The data shown here clearly exhibit a significant scatter of up to 3-4 GPa. This scatter of the different data sets and measurements is more significant than the relative error of each pressure point itself. At low pressures it can be attributed to different packing fraction within the gasket chamber and thus different onset of pressure increase. At higher pressures it is more likely correlated to the different times/pressures at which the conversion from the hard diamond cubic to the very soft metallic phase was completed in each case. The pressure-load curves presented here are thus relevant and applicable to Si and Ge and the syntheses described below. Further measurements may be required for different samples without such drastic transitions or different mechanical properties. However, good agreement is obtained with silica glass (which lacks such transitions), as described elsewhere by Guerette *et al.*.

Examples of the *in situ* diffraction data from crystalline dc-Ge in our anvils compared to data from double-toroidal anvils are shown in Fig 3. Thereby, the double-toroidal experiment utilized TiZr gaskets and was set-up in the standard vertical configuration in the VX3 press. As expected, the Ge sample signal with respect to the PCD anvils is significantly higher in the double-toroidal set-up due to the larger sample exposed and fact that the beam does not enter through the PCD anvil. In the case of the our design it is thus necessary to subtract an empty cell for background. It should be noted, however, that during this test the double-toroidal set-up blew out at 120 t, or 10.5 GPa, well before the dc-Ge had fully transformed to (β-Sn)-Ge. Despite the better sample statistics, the metallization of Ge is thus not easily observable with the double toroidal design on SNAP.

4. *Ex situ* neutron characterization of high pressure synthesized material

The volume of material created using our anvils is sufficient for total neutron scattering on NOMAD and for neutron spectroscopy on VISION. This is demonstrated here on the example of amorphous germanium (a-Ge).

Pure amorphous Ge, just like amorphous Si, is regarded as model systems for all covalently bonded tetrahedral disordered networks [29–31]. The structure of the lowest-energy

amorphous state, the so-called relaxed state that results from sufficient thermal annealing, is most commonly regarded as a prototype of a fully bonded continuous random network. Open questions remain, however, and the exact structure is under debate. Furthermore, a-Si and a-Ge exhibit a very strong structural diversity with many different amorphous structures possible depending on the formation method. For details see for example Refs. [30–35] and Refs. therein. This structural diversity is poorly characterized and not well understood.

Many of the open questions in regards to a-Si's and a-Ge's structure are in part due to the fact that it has been difficult to synthesize large volumes of pure a-Si or a-Ge. Such forms can only be made through solid-state amorphization from entirely pure crystalline precursor materials rather than via deposition techniques (which yield significant impurity levels, specifically of hydrogen, oxygen and carbon). Indeed, the main body of work on pure a-Si and a-Ge described above relies on ion-implantation which creates pure amorphous films of a few μm thickness only. This sample volume limitation can be overcome through the high pressure, low temperature synthesis performed here which allowed us to obtain volumes of $\sim$2 mm^3 of pure material.

Pure a-Si and a-Ge can be made from their crystalline diamond-cubic counterparts by a low temperature, decompression pathway [36–38]. The first step requires the full metallization of Si and Ge at 77 K. This can be achieved either through room temperature compression to $\sim$15 GPa to achieve full conversion to the (β-Sn) phases followed by cooling. Alternatively, compression at 77 K also yields metallic phases, (β-Sn)-Ge and sh-Si, albeit at the slightly elevated pressures. Subsequent decompression of the (β-Sn) structures at 77 K, yields no four-fold coordinated phases (metastable or stable), Instead the six-fold coordinated (β-Sn) configuration persists even upon full pressure release. Upon warming to room temperature, these (β-Sn) phases transform to an amorphous structure. This thus represents a solid-state amorphization pathway for the synthesis of entirely pure a-Si and a-Ge.

Two a-Ge syntheses were performed with portions of pellets from finely ground dc-Ge powder as starting material. To ensure best possible filling, some extra material was piled on top and the gasket was compressed to 0.5 t between the anvils. The anvil/gasket set-up was loaded into the VX5 and pressurized to 40 t (600 bar) while remaining at room temperature.

For the first run (Ge #1), the anvils were cooled to 89.2 K using SNAP's VX5 copper cooling clamps. Decompression then followed slowly over $\sim$30 mins whereby the anvils cooled down further to 83.6 K. Thereafter, the sample returned to room temperature over night[1]. For a second run (Ge #2), the sample was kept at 40 t for 1 h after full compression. Following cooling, the sample was kept at 40 t and 80 K for another 2 h. After decompression to 1 bar, the sample was kept at 80 K for another 2 h. Then warming to room temperature followed. Following these high pressure syntheses, the materials were removed from the gaskets.

Ge #1 was placed into a 2 mm glass capillary for study on NOMAD. Ge #2 was wrapped into Al foil for study on VISION. Following measurement of the as-prepared a-Ge, the structure of Ge #2 was fully relaxed via thermally annealing to 365° for 10 mins [30] under vacuum in a 2 mm glass capillary in a tube furnace. The resulting relaxed a-Ge was then studied on both, NOMAD and VISION.

The NOMAD beamline is a neutron powder diffraction instrument dedicated to the study of local order in nanoscaled-ordered materials [20] and specifically small samples. Thus, the $\sim$2 mm^3 of a-Ge were detected within $\sim$15 mins. To obtain good quality total

[1]Note that for this run, no pre-compressed gasket with a remaining rim was used but instead a gasket with a 2.5 mm hole, i.e. the same size as the dimple. This resulted in such extrusion of the gasket material that the gasket material cracked. Therefore, the approach with a stabilizing rim was adopted, thereafter.

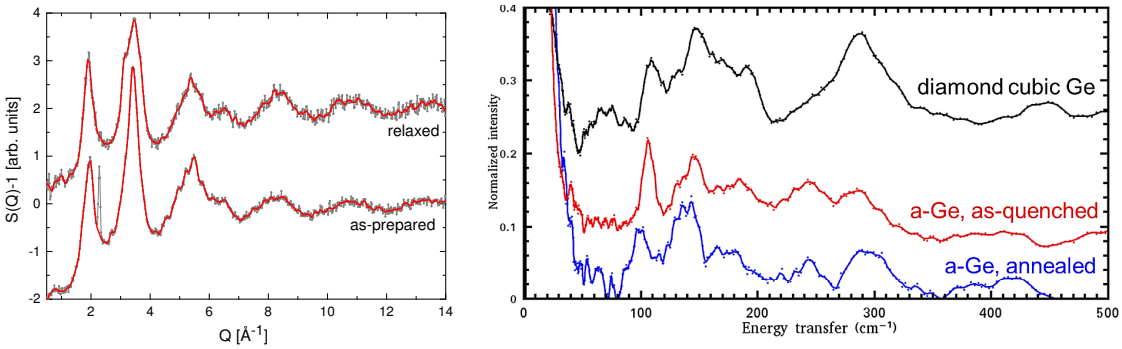

Figure 4. (Colour online) *Ex situ* neutron characterization of as-prepared and relaxed (thermally annealed) a-Ge made by low-temperature decompression [36]. (a) Neutron diffraction from NOMAD yields detailed S(Q), whereby the relaxed data set is offset by a factor of 2 for clarity. For both a-Ge materials, the original data sets obtained from reduction on NOMAD (gray) are given together with the results of a 13-point Savitzky-Golay smoothing routine (red). In the as-prepared case a crystalline diffraction peak at 2.28 å$^{-1}$ originating from metastable Ge phases was removed before smoothing. (b) Inelastic neutron scattering of the two forms of a-Ge and of dc-Ge taken on VISION gives detailed vibrational properties.

scattering data, a long scan of 12 h together with a scan of the empty capillary of the same length was conducted. The exact same capillary at the same location was used for both these scans. The standard instrument calibration (empty instrument, vanadium in instrument and vanadium in glass capillary) was used to normalize the sample data. The resulting structure factors $S(Q)$ of as-prepared and thermally relaxed a-Ge are shown in Fig. 4(a).

Neutron spectroscopy gives unique insight into a material's vibrational properties. In contrast to optical spectroscopy, selection rules do not apply and vibrational spectra can be easily computed analytically. The same sample volumes of $\sim$2 mm^3 of as-prepared and relaxed a-Ge were also measured on VISION [21] and the resulting spectra are shown in Fig. 4(b). Clear differences between the two states of a-Ge are observed which demonstrates that vibrational characteristics of different forms of a-Ge on such a small sample volume are indeed detected.

Note that a full analysis of the structural differences and details of these two forms of a-Ge facilitated by these current measurements is outside the scope of this manuscript here and will be presented elsewhere.

5. Rate control for more variable synthesis parameters

To further optimize synthesis of a-Ge and also a-Si, improved control over decompression rates available was utilized. Specifically, Si undergoes amorphization upon rapid pressure release from metallic phases at room temperature. This has been specifically well studied for the small volume compressed during point loading [33]. In this latter case, sample volumes are however many orders of magnitude smaller. To achieve the same amorphization result with the large volume anvils, the combination of low temperature and rapid decompression is clearly the most promising avenue.

Thus, several single crystal pieces (5-10) of Si and Ge (University wafer, (100), p-doped to 1-10 Ωcm^{-1} and undoped with $\geq$50 Ωcm^{-1}, respectively) were stacked into the gaskets and pressurized to 40 t in the VX5. To ensure full conversion to metallic phases, the material was left under pressure for at least 1 h. Thereafter, the anvils were cooled directly by pouring liquid nitrogen into the modified backing plate with the cryogenic reservoir (see Fig. 1(b)). This yielded an anvil temperature of 100 K after $\sim$20 mins. While keeping the anvils at this temperature, the pressure was released rapidly from the sample by first isolating the PE press from the hydraulic pump, then decompressing the hydraulic

pump. Once fully decompressed, the vent was opened to release any pressure from the PE press within ∼1 s. Thereafter, the sample was allowed to warm to room temperature. 3 synthesis runs were performed for a-Ge and 4 for a-Si using these somewhat abusive conditions on the anvils.

The number of synthesis runs possible allowed us to thermally anneal a portion of the a-Ge samples (at 365° for 10 mins) and of the a-Si samples (at 450° for 30 mins) to fully relax the respective structures to the lowest energy state of pure a-Si and a-Ge [30, 33]. These samples were taken for successful X-ray total scattering studies at beamline 6-ID-D at the Advanced Photon Source (APS) at Argonne National Laboratory (data not shown here), which confirmed that amorphous samples had been created. While samples of similar sizes have been synthesized in toroidal-type pressure devices before, only 50% and 80% amorphous fractions were obtained for Si and Ge, respectively [37]. Thus, these samples here represent most likely the largest volumes of relaxed a-Si and a-Ge synthesized to date.

Clearly, the anvil design described here allows for synthesis of sufficient volumes of pure a-Si and a-Ge to be used for further *ex situ* characterization techniques. This is not limited to neutron (or X-ray) diffraction and vibrational spectroscopy but can also be extended to the many characterization techniques commonly used in solar cell and other optoelectronic materials research. Finally, the synthesis capability are clearly not limited to a-Si and a-Ge and may be of interest in the wide-spread search for recoverable metastable phases.

6. Future developments

The modified Bridgman design described here exhibits much potential for further development. For example, although the VX5 was used for the experiments presented here, the significantly smaller VX1 press also achieves 40 t and thus 20 GPa with these anvils. The smaller size of the VX1 may allow for easier cooling and is also more portable. This may enable higher ease of complementary experiments such as neutron diffraction and spectroscopy but potentially also complementary X-ray diffraction.

Moreover, the current anvil and gasket design proved extremely reliable and stable as all experiments presented here were performed on the exact same set of anvils. Further room temperature pressurizations to ∼20 GPa not described here were performed to a total of 20. During the last run, the anvil chipped somewhat at the edge of the 'dimple' but did not fully break. This impressive reliability of the design is crucial for synthesis but may also allow extension to weaker anvil and gasket materials such as cBN anvils and TiZr gaskets. Use of the same gasket design (i.e. with a rim to prevent extrusion and encourage gasket flow toward the sample centre), may conceivable allow for similar pressures with these anvils and gaskets. This clearly would allow for exploitation of the advantages provided by cBN anvils/TiZr gaskets such as absence of gasket peaks and self-collimating anvils.

Finally, the current anvil/gasket design has not been taken to the breaking point yet. Based on the number of runs successfully performed on one anvil set, it will clearly be possible to extend the pressure regime beyond 20 GPa. This will be explored on a new set of anvils without hole at the back and using solid backing plates. Although such a design is not well compatible with the horizontal geometry used for *in situ* diffraction on SNAP at 60 Hz described here, it will be very viable for offline synthesis. Additionally, the anvils can also be placed in the vertical geometry online on SNAP which would allow for the entire d-range available to SNAP upon movement of the detectors. Although gasket steel peaks would be present, these would not overlap with diffraction peaks at high d. Thus, the study of magnetic peaks, for example, or also EoS measurements with

pressure calibrants such as NaCl could be facilitated.

7. Conclusion

Here we report on a modified Bridgman design for anvils used in a Paris-Edinburgh press. The design consists of a simple 'dimple' used together with pre-formed steel gaskets. Using this set-up yields in $\sim$2 mm^3 of synthesized sample volume, sufficient for *in situ* diffraction on SNAP but also for *ex situ* neutron diffraction and spectroscopy. Key advantages lie in the facts (i) that application of 40 t already achieves a pressure of 20 GPa, (ii) that rapid decompression can be safely used, (iii) that easy cooling with liquid nitrogen is possible, (iv) that materials with large volume changes upon phase transition do not pose a challenge, and (v) that the design is highly reliable with 20 pressure runs to 20 GPa performed on the same anvil set. While this design has been largely used for synthesis of amorphous Si and Ge here, it clearly would also be adaptable to other syntheses or also for *in situ* diffraction on materials with long d-spacings of interest.

Acknowledgments

The authors gratefully acknowledge highly helpful discussion with Malcolm Guthrie (ESS, Sweden) throughout this work. BH acknowledges funding through a Weinberg Fellowship sponsored by the Laboratory Directed Research and Development Program of Oak Ridge National Laboratory, managed by UT-Battelle, LLC, for the U. S. Department of Energy. RB was partially supported by EFree, an Energy Frontier Research Center funded by the U.S. Department of Energy, Office of Science, Basic Energy Sciences under Award No. DE-SC0001057. Research was conducted at three beamlines of ORNL's Spallation Neutron Source, SNAP, NOMAD and VISION, all supported through DOE-BES's Scientific User Facilities division.

References

[1] Squires GL. Introduction to the Theory of Thermal Neutron Scattering. Dover Publications; 1997.
[2] Khvostantsev L, Slesarev V, Brazhkin V. Toroid type high-pressure device: History and Prospects. High Pressure Research. 2004;24:371–383.
[3] Klotz S. Techniques in high pressure neutron scattering. Boca Raton (FL, USA): CRC Press - Taylor and Francis Group; 2013.
[4] Klotz S, Besson J, Hamel G, Nelmes R, Loveday J, Marshall W, Wilson R. Neutron powder diffraction at pressures beyond 25 GPa. Applied Physics Letters. 1995;66:1735.
[5] Klotz S, Strässle T, Lebert B, d'Astuto M, Hansen T. High pressure neutron diffraction to beyond 20 GPa and below 1.8 K using Paris-Edinburgh load frames. High Pressure Research. 2016;36:73–78.
[6] Iizuka R, Yagi T, Gotou H, Komatsu K, Kagi H. An opposed-anvil-type apparatus with an optical window and a wide-angle aperture for neutron diffraction. High Pressure Research. 2012;32:430–441.
[7] Komatsu K, Klotz S, Shinozakia A, Iizukaa R, Bove L, Kagi H. Performance of ceramic anvils for high pressure neutron scattering. High Pressure Research. 2014;34(4):494–499.
[8] Liebermann R. Multi-anvil, high pressure apparatus: a half century of development and progress. High Pressure Research. 2011;31:493–532.
[9] Yamazaki D, Ito E, Yoshino T, Tsujino N, Yoneda A, Guo X, Xu F, Higo Y, Funakoshi K. Over 1 Mbar generation in the Kawai-type multianvil apparatus and its application

to compression of $(Mg_{0}.92Fe_{0}.08)SiO_3$ perovskite and stishovite. Physics of the Earth and Planetary Interiors. 2014;228:262–267.

[10] Abe J, Arakawa M, Hattori T, Arima H, Kagi H, Komatsu K, Sano-Furukawa A, Uwatoko Y, Matsubayashi K, Harjo S, Moriai A, Ito T, Aizawa K, Arai M, Utsumi W. A cubic-anvil high-pressure device for pulsed neutron powder diffraction. Review of Scientific Instruments. 2010;81:043910.

[11] Sano-Furukawa A, Hattori T, Arima H, Yamada A, Tabata S, Kondo M, Nakamura A, Kagi H, Yagi T. Six-axis multi-anvil press for high-pressure, high-temperature neutron diffraction experiments. Review of Scientific Instruments. 2014;85:113905.

[12] Osakabe T, Kakurai K, Kawana D, Kuwahara K. Development of a hybrid-anvil type high-pressure device and its application to magnetic neutron scattering studies. Journal of Magnetism and Magnetic Materials. 2007;310:2725–2727.

[13] Osakabe T, Kuwahara K, Kawana D, Iwasa K, Kikuchi D, Aoki Y, Kohgi M, Sato H. Pressure-induced antiferromagnetic order in filled skutterudite prfe4p12 studied by single-crystal high-pressure neutron diffraction. Journal of the Physical Society of Japan. 2010; 79(3):034711.

[14] Goncharenko I, Loubeyre P. Neutron and x-ray diffraction study of the broken symmetry phase transition in solid deuterium. Nature. 2005;435:1206–1209.

[15] Goncharenko IN. Neutron diffraction experiments in diamond and sapphire anvil cells. High Pressure Research. 2004;24:193–205.

[16] Boehler R, Guthrie M, Molaison J, dos Santos A, Sinogeikin S, Machida S, Pradhan N, Tulk C. Large-volume diamond cells for neutron diffraction above 90 GPa. High Pressure Research. 2013;33:546–554.

[17] Boehler R, Molaison J, Haberl B. Novel Diamond Cells for Neutron Diffraction using multi-carat CVD Anvils. 2017. manuscript submitted to Review of Scientific Instruments.

[18] Haberl B, Dissanayake S, Ye F, Daemen LL, Cheng Y, Li CW, Ramirez-Cuesta AJT, Matsuda M, Molaison JJ, Boehler R. Wide-angle diamond cell for neutron scattering. High Pressure Research. 2017;37:495.

[19] Calder S, An L, Boehler R, Cruz CD, Frontzek M, Guthrie M, Haberl B, Huq A, Kimber A, Molaison J, Neuefeind J, Page K, dos Santos A, Tulk C, Tucker M. A suite-level review of the neutron powder diffraction instruments at Oak Ridge National Laboratory. Review of Scientific Instruments. 2018;xx:xxx.

[20] Neuefeind J, Feygenson M, Carruth J, Hoffmann R, Chipley KK. The Nanoscale Ordered MAterials Diffractometer NOMAD at the Spallation Neutron Source SNS. Nuclear Instruments and Methods in Physics Research B. 2012;287:68–75.

[21] Seeger PA, Daemen LL, Larese JZ. Resolution of VISION, a crystal-analyzer spectrometer. Nuclear Instruments and Methods in Physics A. 2009;604:719–728.

[22] Jamieson JC. Crystal structures at high pressures of metallic modifications of silicon and germanium. Science. 1963;139:762–764.

[23] Arnold O, Bilheux JC, Borreguero JM, Buts A, Campbell SI, Chapon L, Doucet M, Draper N, Leal RF, Gigg MA, Lynch VE, Markvardsen A, Mikkelson DJ, Mikkelson RL, Miller R, Palmen K, Parker P, Passos G, Perring TG, Peterson PF, Ren S, Reuter MA, Savici AT, Taylor JW, Taylor RJ, Tolchenov R, Zhou W, Zikovsky J. Mantid Data analysis and visualization package for neutron scattering and μSR experiments. Nuclear Instruments and Methods in Physics Research Section A: Accelerators, Spectrometers, Detectors and Associated Equipment. 2014;764:156–166.

[24] Vohra Y, Ruoff A. Static compression of metals Mo, Pb, and Pt to 272 GPa: Comparison with shock data. Physical Review B. 1990;42:8651.

[25] Pandya TC, Thakar NA, Bhatt AD. Analysis of equations of state and temperature dependence of thermal expansivity and bulk modulus for silicon. Journal of Physics: Conference Series. 2012;377:012097.

[26] Mujica A, Rubio A, Munõz A, Needs RJ. High-pressure phases of group-IV, III-V, and II-VI compounds. Reviews of Modern Physics. 2003;75(3):863–912.

[27] Olijnyk H, Sikka SK, Holzapfel WB. Structural phase transitions in Si and Ge under pressures up to 50 GPa. Physics Letters. 1984;103A(3):137–140.

[28] Gupta MC, Ruoff AL. Static compression of silicon in the [100] and in the [111] directions.

Journal of Applied Physics. 1980;51(2):1072–1075.
[29] Polk DE. Structural model for amorphous silicon and germanium. Journal of Non-Crystalline Solids. 1971;5(5):365–376.
[30] Roorda S, Martin C, Droui M, Chicoine M, Kazimirov A, Kycia S. Disentangling neighbors and extended range density oscillations in monatomic amorphous semiconductors. Physical Review Letters. 2012;108:255501.
[31] Holmström E, Haberl B, Pakarinen OH, Nordlund K, Djurabekova F, Arenal R, Williams JS, Bradby JE, Petersen TC, Liu ACY. Dependence of short and intermediate-range order on preparation in experimental and modeled pure a-Si. Journal of Non-Crystalline Solids. 2016;438:26–36.
[32] Fortner J, Lannin JS. Structural relaxation and order in ion-implanted Si and Ge. Physical Review B. 1988;37(17):10154–10158.
[33] Haberl B, Liu ACY, Bradby JE, Ruffell S, Williams JS, Munroe P. Structural characterization of pressure-induced amorphous silicon. Physical Review B. 2009;79:155209.
[34] Laaziri K, Kycia S, Roorda S, Chicoine M, Robertson JL, Wang J, Moss SC. High-energy X-ray diffraction study of pure amorphous silicon. Physical Review B. 1999;60(19):13520–13533.
[35] Roorda S, Sinke WC, Poate JM, Jacobson DC, Dierker S, Dennis BS, Eaglesham DJ, Spaepen F, Fuoss P. Structural relaxation and defect annihilation in pure amorphous silion. Physical Review B. 1991;44(8):3702–3725.
[36] Imai M, Mitamura T, Yaoita K, Tsuji K. Pressure-induced phase transitions of crystalline and amorphous silicon and germanium at low temperatures. High Pressure Research. 1996; 15:167–189.
[37] Brazhkin VV, Lyapin AG, Popova SV, Voloshin RN. Solid-phase disordering of bulk Ge and Si samples under pressure. Pis'ma Zh Eksp Teor Fiz. 1992;56(3):152–156.
[38] Brazhkin VV, Lyapin AG, Popova SV, Voloshin RN. Non-equilibrium phase transitions and amorphization in Si, Si/GaAs, Ge and Ge/GaSb at the decompression of high pressure phases. Physical Review B. 1995;51(12):7549–7554.